NANO LETTERS

Letter

Linearly Polarized Emission from an Embedded Quantum Dot Using Nanowire Morphology Control

Andrew P. Foster,*,[†] John P. Bradley,[†] Kirsty Gardner,[†] Andrey B. Krysa,[‡] Ben Royall,[†] Maurice S. Skolnick,[†] and Luke R. Wilson*,[†]
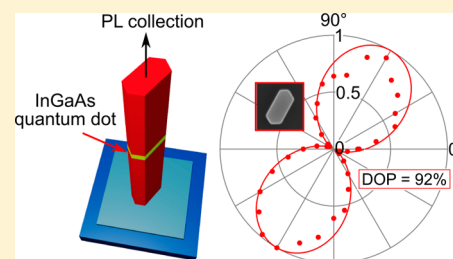
[†]Department of Physics and Astronomy, University of Sheffield, Sheffield S3 7RH, United Kingdom
[‡]Department of Electronics and Electrical Engineering, University of Sheffield, Sheffield S1 3JD, United Kingdom

S Supporting Information

ABSTRACT: GaAs nanowires with elongated cross sections are formed using a catalyst-free growth technique. This is achieved by patterning elongated nanoscale openings within a silicon dioxide growth mask on a (111)B GaAs substrate. It is observed that MOVPE-grown vertical nanowires with cross section elongated in the $[2\bar{1}\bar{1}]$ and $[\bar{1}12]$ directions remain faithful to the geometry of the openings. An InGaAs quantum dot with weak radial confinement is realized within each nanowire by briefly introducing indium into the reactor during nanowire growth. Photoluminescence emission from an embedded nanowire quantum dot is strongly linearly polarized (typically >90%) with the polarization direction coincident with the axis of elongation. Linearly polarized PL emission is a result of embedding the quantum dot in an anisotropic nanowire structure that supports a single strongly confined, linearly polarized optical mode. This research provides a route to the bottom-up growth of linearly polarized single photon sources of interest for quantum information applications.

KEYWORDS: nanowire, quantum dot, morphology control, linear polarization, photon source

Bottom-up growth techniques provide a versatile platform for the development of nanowire photon sources. The advantages of such an approach include the ability to embed within the nanowire quantum dots (NWQDs) exhibiting very narrow exciton line widths[1] and to use lithographic definition of the nanowire growth sites to enable position controlled single photon sources.[2−4] Significant progress has been made in tailoring the optical emission properties of NWQDs, for instance through deliberate tapering of the nanowire to achieve a Gaussian emission profile with very high optical fiber collection efficiency.[5] Growth of an on-axis NWQD can be utilized to enable a high single photon emission rate by ensuring the host nanowire has correct dimensions to support a single well confined optical mode.[6]

Epitaxially grown semiconductor nanowires most commonly exhibit a quasicylindrical symmetry, within the limits determined by the crystalline side facets developed during the growth process. A previous report of epitaxially grown nanowires with alternative cross-sectional geometries involved the use of dopants to alter the morphology of a nanowire shell during radial overgrowth.[7] An alternative technique to develop nanowires with anisotropic cross section utilizes top-down etching,[8] although this cannot produce the high quality nanowire facets enabled by nanowire growth nor can it easily allow for radial overgrowth of a shell passivation layer to reduce the rate of nonradiative recombination via surface states. Bottom-up growth also allows for positional control both of a NWQD on the axis of the nanowire, and the nanowires themselves through the use of lithographic definition of nanowire nucleation sites.

In this work, we demonstrate for the first time morphological control of a nanowire using the catalyst-free, selective-area growth technique that can be achieved without resorting to doped radial nanowire growth. By patterning elongated holes (nanoslots) in a dielectric growth mask on a (111)B GaAs wafer, we enable the epitaxial growth of vertical nanowires with elongated cross section. An InGaAs NWQD is embedded within each nanowire and InGaAs photoluminescence (PL) emission collected from the top facet of the nanowire is observed to exhibit strong linear polarization. Ultimately, this provides a route for the bottom-up growth of linearly polarized single photon sources, with potential applications as sources for quantum information processing.[8,9]

Nanowire sample fabrication commenced with plasma enhanced chemical vapor phase deposition of ∼30 nm of SiO_2 on a (111)B GaAs substrate. The SiO_2 was patterned into squares of side length 135 μm in order to moderate the nanowire growth rate.[10] Square arrays of nanoslots with a pitch of 4 μm were patterned into each SiO_2 square using a combination of electron beam lithography and reactive ion etching. The nanoslots had a designed aspect ratio of 2:1, with the smallest experimentally realized having major (minor) axis

length of 200 nm (90 nm). During the catalyst-free growth of GaAs nanowires, six {110} facets develop to form the side facets parallel to the growth axis of the nanowire due to their much slower growth rate compared to the (111)B top facet.[11] These provide limitations on the nanoslot orientations which may be best used to grow elongated cross section nanowires, as shown in Figure 1. There are six most logical elongation
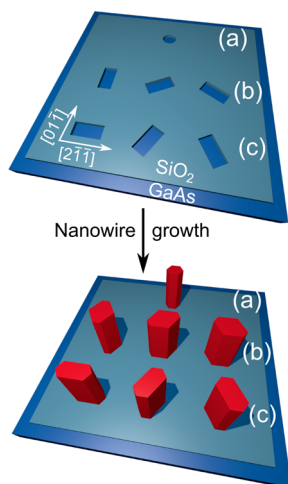

Figure 1. (a) (Top) Nanohole patterned into the SiO_2 dielectric leads to (Bottom) growth of a regular hexagonal nanowire with (110) facets; (b) nanoslots elongated along $[01\bar{1}]$, $[10\bar{1}]$, and $[\bar{1}10]$ lead to growth of elongated nanowires with low cross section aspect ratio; (c) nanoslots elongated along $[2\bar{1}\bar{1}]$, $[\bar{1}12]$, and $[\bar{1}2\bar{1}]$ lead to growth of elongated nanowires with high cross-sectional anisotropy.

directions. Of these, those orientated along the $[01\bar{1}]$, $[10\bar{1}]$, and $[\bar{1}10]$ directions lead to the growth of weakly anisotropic nanowires (Figure 1b). Those along the $[2\bar{1}\bar{1}]$, $[\bar{1}12]$, and $[\bar{1}2\bar{1}]$ directions, however, lead to the growth of strongly anisotropic nanowires (Figure 1c).

With the nanowire faceting in mind, elongation directions along $[2\bar{1}\bar{1}]$, $[\bar{1}12]$, and $[01\bar{1}]$ were utilized. The latter, which produces a nanowire with weakly anisotropic cross section, was included to enable comparison of both weak and strong anisotropy in the nanowire cross section. Scanning electron microscope (SEM) images of representative nanoslots are shown in Figure 2b,d,f. Prior to growth, the substrate was briefly dipped in 1% HF to remove residual SiO_2 from within the nanoslots. This was found to significantly improve the uniformity of the resulting nanowire arrays.

GaAs nanowires were grown using low-pressure MOVPE at 750 °C. After annealing the sample for 9 min at 780 °C to remove oxides of gallium and arsenic from the nanoslots, growth was undertaken using TMGa and AsH_3 precursors with flows of 33 and 15 sccm, respectively. After 180 s of GaAs growth, TMIn was introduced into the reactor, while maintaining the flow of TMGa and AsH_3. To maximize the likelihood of realizing an optically active InGaAs NWQD within the nanowire, the two growth steps above were repeated four times, with the conditions for each InGaAs NWQD varied. We found that this procedure typically led to the realization of a single optically active NWQD. The first two InGaAs NWQDs were grown with a TMIn concentration of 0.02% in a total H_2 flow of 200 sccm with growth times of 2 s and 4 s, respectively. The final two structures had growth times of 2 s and 4 s respectively, with a TMIn concentration of 0.04% in 200 sccm
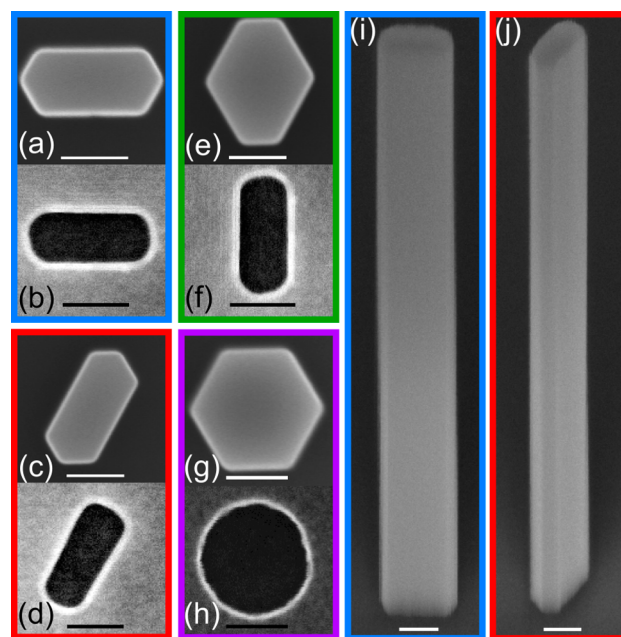

Figure 2. SEM images of nanoslots formed in the (b) $[2\bar{1}\bar{1}]$, (d) $[\bar{1}12]$, and (f) $[01\bar{1}]$ directions and (h) a regular nanohole. Rounded corners in (b,d,f) are an artifact of the EBL patterning and etching conditions. Top down SEM images of vertical nanowires grown with cross section elongation in the (a) $[2\bar{1}\bar{1}]$, (c) $[\bar{1}12]$, and (e) $[01\bar{1}]$ directions, and (g) with no elongation of the cross section. The 45° tilted SEM images of nanowires grown in the (i) $[2\bar{1}\bar{1}]$ and (j) $[\bar{1}12]$ directions. All scale bars 100 nm.

of H_2. Finally, 90 s of GaAs growth was used to cap the uppermost InGaAs NWQD. The sample was cooled under an overpressure of PH_3 and AsH_3 with flow rates of 300 and 150 sccm respectively, to prevent degradation of the nanowires and ideally provide a degree of surface passivation through phosphorus−arsenic exchange at the nanowire surface.

Figure 2 shows representative SEM images of the final untapered nanowires. It can be seen that nanowires grown with cross section elongation in the $[2\bar{1}\bar{1}]$ and $[\bar{1}12]$ directions maintained the geometry of the underlying nanoslots, whereas those grown along the $[01\bar{1}]$ direction showed an unavoidable variation from the nanoslot pattern due to the facet-led growth process. The narrowest nanowires grown had a major (minor) axis length of ∼200 nm (∼100 nm) and heights of ∼2 μm. The growth procedure therefore led to predominantly axial growth, with a radial growth thickness of only ∼10 nm. The InGaAs NWQDs formed within such a nanowire had heights of ∼5 nm and ∼10 nm based on a linear growth rate approximation (for 2 s and 4 s growth times respectively), whereas the GaAs barrier between each NWQD was ∼440 nm thick. For comparison, it was confirmed that nanowires grown from circular openings had a regular hexagonal cross section, as shown in Figure 2g,h. The high density of rotational twins observed using our growth conditions precluded the use of TEM to observe the formation of NWQDs within the nanowires.[2]

PL measurements at ∼5 K were undertaken using linearly polarized laser excitation at 633 nm, with each nanowire addressed individually in the vertical geometry. The polarization of the laser was found to have no influence on the experimental results. The laser was focused to a ∼2 μm spot using a 50× microscope objective with an NA of 0.42. PL from each NWQD was collected using the same objective, dispersed

using a spectrometer and accumulated using a nitrogen-cooled CCD. For polarization-resolved PL, a linear polarizer with high extinction ratio ($>10^8$) and a half-wave plate were placed in the collection path. The latter was used to account for the polarization sensitivity of the spectrometer grating.

NWQD PL emission was observed from ~75% of nanowires on the sample. Unless stated otherwise, the following results are for the narrowest nanowires grown, as discussed above. In general, a single PL emission line was observed at low excitation power (~1 nW) for the narrowest nanowires, suggesting that only one of the four InGaAs NWQDs was optically active in these nanowires. This implies that improvements could be made in future to the growth process to increase the rate of successful NWQD formation. Figure 3a shows representative
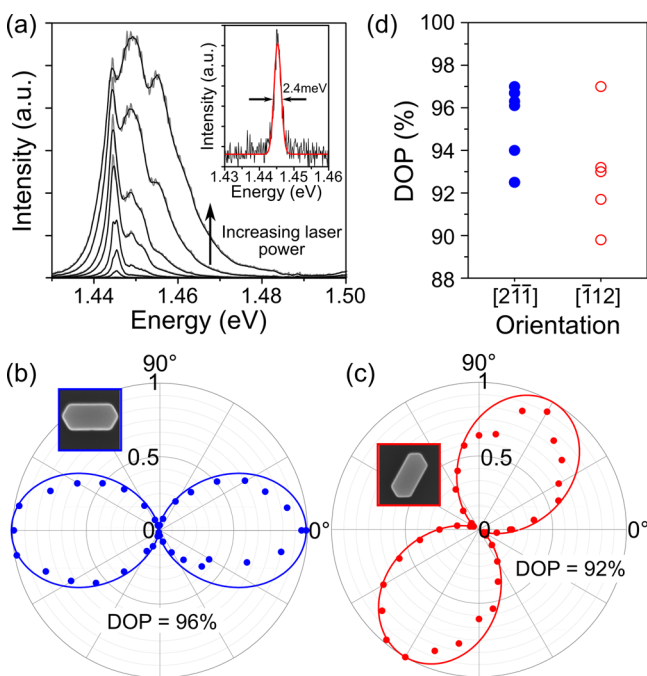

Figure 3. (a) Power-dependent NWQD PL spectra taken from a single nanowire elongated along the $[2\overline{1}\overline{1}]$ direction, with three confined states visible at the highest laser power (gray line, raw data; black line, smoothed data). (Inset) Ground state NWQD PL spectrum (black line) with Gaussian fit to data (red line). Normalized, polarization-resolved NWQD PL intensity for nanowires with cross section elongated in the (b) $[2\overline{1}\overline{1}]$ and (c) $[\overline{1}12]$ directions. Circles represent measured data points, solid lines show sine curve fits to the data. Insets provide a reminder of the nanowire orientations. (d) Degree of polarization statistics for nanowires with cross section elongated in the $[2\overline{1}\overline{1}]$ and $[\overline{1}12]$ directions. For definition of DOP see text.

power-dependent PL spectra from a single elongated nanowire with major axis orientated along the $[2\overline{1}\overline{1}]$ direction. At low power, a single emission line can be seen at 1.445 eV, whereas at higher powers (up to ~1 μW), the filling of NWQD excited states can be observed. This behavior is expected for PL emission from a NWQD. The state separation of ~3.6 meV is somewhat larger than expected from a simple model of the NWQD as a square infinite potential well (~1 meV) and supports our previous observations using this growth technique.[2] This was previously attributed to a reduction in the incorporation of indium across the width of the nanowire, resulting in increased lateral confinement of carriers due to the

change in bandgap across the width of the NWQD and leading to NWQD formation verified by the single photon character of the observed PL emission.

Polarization-dependent PL measurements were taken at the saturation point of the NWQD ground state transition to maximize the PL signal (typical excitation powers ~50−100 nW). Figure 3b and c show polarization resolved measurements for nanowires orientated in the $[2\overline{1}\overline{1}]$ and $[\overline{1}12]$ directions, respectively. The PL emission can be seen to be strongly linearly polarized with an axis of polarization coincident with the elongated axis of the nanowire. In contrast, NWQDs in nanowires orientated along the $[01\overline{1}]$ direction showed weak and random polarization, attributed to the much smaller aspect ratio of the these nanowires compared to those formed along the $[2\overline{1}\overline{1}]$ and $[\overline{1}12]$ directions. This was also seen to be the case for regular hexagonal nanowires, an observation that has been made previously for InAsP NWQDs in InP nanowires.[12]

We quantify the degree of linear polarization (DOP) using the ratio DOP = $(I_{max} - I_{min})/(I_{max} + I_{min})$, where I_{max} is the integrated PL intensity measured with polarization parallel to the elongation axis of the nanowire, and I_{min} the intensity measured with polarization perpendicular to this. Figure 3d summarizes the DOP for six nanowires in each of the $[2\overline{1}\overline{1}]$ and $[\overline{1}12]$ directions. For nanowires elongated in the $[2\overline{1}\overline{1}]$ direction, the DOP was found to be 95 ± 1%, while for the $[\overline{1}12]$ direction it was 93 ± 1%.

Polarized NWQD emission from an elongated cross section nanowire is the result of the InGaAs PL emission coupling to a single linearly polarized optical mode of the nanowire. A regular hexagonal GaAs nanowire with diameter less than ~260 nm operates in the single optical mode regime, supporting two weakly nondegenerate fundamental optical modes for emission energy of 1.445 eV ($\lambda \sim 860$ nm). The dispersion relationship for the fundamental modes of a nanowire of 210 nm diameter is shown in Figure 4a. At an energy of 1.445 eV the dispersion of the guided modes lies well away from the light line, indicating the high degree of confinement of the modes to the nanowire. Also shown are the electric field profiles of the optical modes (insets of Figure 4a), which are seen to be orthogonally polarized. Given that a NWQD may be modeled as a dipole orientated perpendicularly to the nanowire axis,[13,14] emission from an on-axis dipole would occur equally into each mode, resulting in unpolarized light emission.

Growing nanowires with an elongated cross section significantly increases the nondegeneracy of the two modes. This results in two linearly polarized optical modes orientated parallel and perpendicular to the axis of elongation. Tuning the major and minor axis lengths of the elongated nanowire allows the degree of confinement of each mode within the nanowire to be controlled (note that these are not entirely independent parameters, however). Figure 4b shows the dispersion relationships for the two fundamental optical modes of an infinitely long GaAs nanowire with major (minor) axis lengths of 210 nm (100 nm), the minimum cross section experimentally obtained in this work. These show clearly the difference in modal confinement induced by the nanowire cross-sectional anisotropy. The insets in Figure 4b show the electric field profiles of the fundamental optical modes. It is clear that the mode polarized parallel to the elongation axis of the nanowire is more strongly confined than the orthogonal mode, which is mostly expelled into the air cladding. By choosing conditions for which the mode polarized parallel to the elongation axis is well confined, and the other mode is poorly confined, PL emission
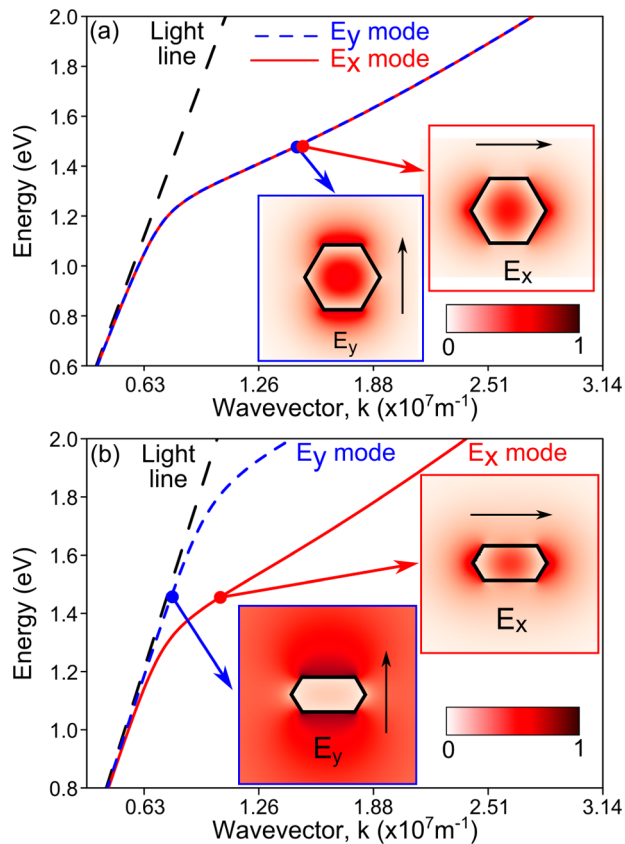
Figure 4. Optical modes in infinite GaAs nanowire waveguides. (a) Weakly nondegenerate, orthogonally polarized fundamental modes in a 210 nm × 182 nm cross section hexagonal waveguide (dashed blue line, y-polarized mode; solid red line, x-polarized mode). Dashed black line shows the light line for free space modes. (Inset) Electric field profiles of the two modes at an energy of 1.445 eV ($\lambda \sim 860$ nm). (b) Strongly nondegenerate orthogonally polarized fundamental modes in an elongated cross section nanowire with major (minor) axis length of 210 nm (100 nm). Dashed blue line, y-polarized mode; solid red line, x-polarized mode. (Inset) Electric field profiles of the x and y polarized modes at 1.445 eV. The x polarized mode is confined to the nanowire, whereas the y polarized mode is excluded, leading to preferential photon emission into the former.

from the InGaAs NWQD is funnelled into the well confined mode, resulting in linearly polarized PL emission from the nanowire. Polarization-resolved PL measurements on nanowires with a cross section of 400 nm by 200 nm, for which both modes were confined within the nanowire, showed a very small DOP as expected from the preceding explanation. We note that in this case the InGaAs emitting region is more accurately described as a quantum well.

Finite difference time domain (FDTD) simulations were undertaken to corroborate the experimental results, using a commercial-grade simulator.[15] The simulation domain is shown in Figure 5a. An elongated cross section nanowire with major (minor) axis length of 210 nm (100 nm) and height of 2 μm was placed above 30 nm of SiO$_2$, on top of a semi-infinite GaAs substrate. A real refractive index of 3.45 was used for the nanowire and the substrate. A broadband dipole emitter was positioned on the nanowire axis at a height d above the substrate. Polarization-resolved far field intensity patterns were obtained for emission from the top facet of the nanowire. This was undertaken separately for a dipole polarized first along the direction of cross section elongation, then perpendicular to this
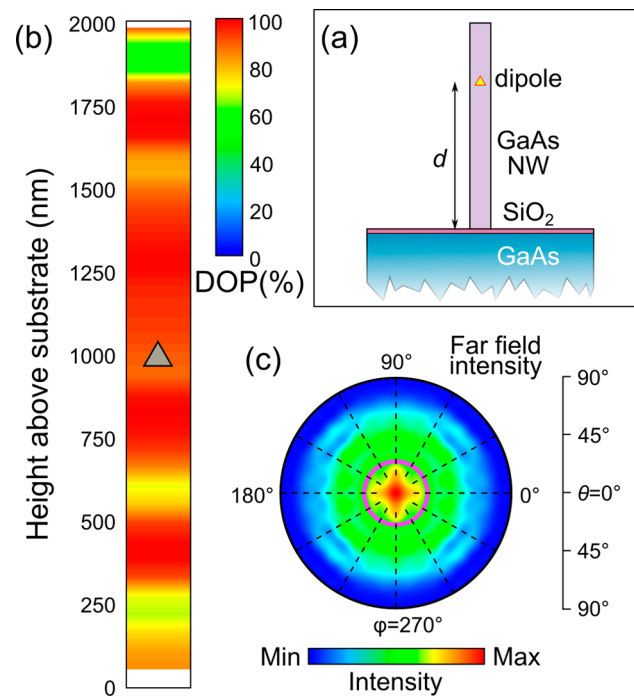

Figure 5. FDTD simulations for an on-axis dipole emitter embedded in an elongated cross section nanowire. (a) Schematic of the simulation domain, with a semi-infinite GaAs substrate. A dipole emitter was placed at a height d above the substrate. The polarization-resolved far field intensity was determined in the vertical direction above the nanowire. (b) DOP as a function of dipole position within the nanowire, for an energy of 1.445 eV ($\lambda \sim 860$ nm). (c) Polarization-resolved far field intensity pattern for $d = 1000$ nm, with the electric field polarized coincident with the elongation direction of the nanowire cross section. The pink circle corresponds to an NA of 0.42, as used in this work. On this scale, the cross-polarized component cannot be observed.

(in both cases perpendicular to the nanowire growth axis), before summing the results. From the far field patterns, the DOP was calculated assuming an objective lens NA of 0.42. Figure 5b shows the DOP as a function of dipole location d, for an emission energy of 1.445 eV ($\lambda \sim 860$ nm). The DOP is greater than 90% for 680 nm < d < 1480 nm, and remains high for almost all values of d. The emission is polarized with electric field orientated along the elongation direction of the nanowire cross section, in agreement with our experimental observations.

The variation in the DOP seen in Figure 5b is the result of weak Fabry–Perot modes forming within the nanowire, plus reflection from the substrate and dipole emission into leaky modes which is particularly evident for a dipole placed near the top of the nanowire. A larger NA objective than used in our experiments would lead to a higher DOP even for dipoles in this location (Supporting Information, Figure S2). Figure 5c shows the polarization-resolved far field emission pattern for a dipole located at $d = 1000$ nm, with the electric field polarized coincident with the elongation direction of the nanowire cross section. It is noted that the cross-polarized far field emission pattern shows no features when plotted on the same scale as Figure 5c, as the emission is much weaker in this case. This obviously results in a high DOP coincident with the elongation axis of the nanowire cross section. We note that although the above analysis is for emission at 860 nm (due to the experimental conditions), polarization control in this manner is inherently broadband, with a DOP greater than 90% in the

wavelength range 860−900 nm calculated for multiple locations within the nanowire (Supporting Information, Figure S2). The analysis also holds in the case of off-axis emission (Supporting Information, Figure S3).

One limitation of the current fabrication procedure lies in the unavoidable growth of a radially large NWQD due to the elongated nature of the nanowire cross section. This leads to a small excited state splitting energy, which may be undesirable for application as a quantum light source. Previously, it was observed that the NWQD diameter as determined from the excited state energy separations was smaller than the physical diameter of the host nanowire.[2] This suggested a reduction in the incorporation of indium across the width of the NWQD, effectively reducing it in size below that of the nanowire. As mentioned previously, this does indeed appear to be the case for elongated nanowires also. An alternative method to fabricate a small on-axis NWQD in an elongated nanowire would be to utilize a combination of catalyzed and catalyst-free growth mechanisms. The catalyst particle could be used to grow a small diameter NWQD at the center of an elongated nanoslot, with the growth mode then switched to the catalyst-free technique to radially cap the nanowire, maintaining the morphology of the nanoslot.

In conclusion, we have demonstrated the selective-area, catalyst-free growth of nanowires with elongated cross section for the first time. InGaAs NWQDs were grown within the nanowires, and NWQD PL emission from the top facet of the nanowires is shown to be strongly linearly polarized (>90%), with the polarization direction being coincident with the elongation axis of the nanowire cross section. This was shown to be a result of the optical modes supported by the nanowires and provides a route to the bottom-up growth of position controlled linearly polarized single photon sources.

■ ASSOCIATED CONTENT

Ⓢ Supporting Information
Schematic of experimental setup, additional FDTD simulation results. This material is available free of charge via the Internet at http://pubs.acs.org.

■ AUTHOR INFORMATION

Corresponding Authors
*E-mail: andrew.foster@sheffield.ac.uk.
*E-mail: luke.wilson@sheffield.ac.uk.
Notes
The authors declare no competing financial interest.

■ ACKNOWLEDGMENTS

■ REFERENCES

(1) Dalacu, D.; Mnaymneh, K.; Lapointe, J.; Wu, X.; Poole, P. J.; Bulgarini, G.; Zwiller, V.; Reimer, M. E. *Nano Lett.* **2012**, *12*, 5919−5923.
(2) Makhonin, M. N.; Foster, A. P.; Krysa, A. B.; Fry, P. W.; Davies, D. G.; Grange, T.; Walther, T.; Skolnick, M. S.; Wilson, L. R. *Nano Lett.* **2013**, *13*, 861−865.
(3) Tatebayashi, J.; Ota, Y.; Ishida, S.; Nishioka, M.; Iwamoto, S.; Arakawa, Y. *Appl. Phys. Lett.* **2012**, *100*, 263101.
(4) Holmes, M. J.; Choi, K.; Kako, S.; Arita, M.; Arakawa, Y. *Nano Lett.* **2014**, *14*, 982−986.
(5) Bulgarini, G.; Reimer, M. E.; Bouwes Bavinck, M.; Jöns, K. D.; Dalacu, D.; Poole, P. J.; Bakkers, E. P. A. M.; Zwiller, V. *Nano Lett.* **2014**, *14*, 4102−4106.
(6) Bulgarini, G.; Reimer, M. E.; Zehender, T.; Hocevar, M.; Bakkers, E. P. A. M.; Kouwenhoven, L. P.; Zwiller, V. *Appl. Phys. Lett.* **2012**, *100*, 121106.
(7) Kim, S.-K.; Day, R. W.; Cahoon, J. F.; Kempa, T. J.; Song, K.-D.; Park, H.-G.; Lieber, C. M. *Nano Lett.* **2012**, *12*, 4971−4976.
(8) Munsch, M.; Claudon, J.; Bleuse, J.; Malik, N. S.; Dupuy, E.; Gérard, J.-M.; Chen, Y.; Gregersen, N.; Mørk, J. *Phys. Rev. Lett.* **2012**, *108*, 077405.
(9) Lundskog, A.; Hsu, C.-W.; Karlsson, K. F.; Amloy, S.; Nilsson, D.; Forsberg, U.; Holtz, P. O.; Janzen, E. *Light Sci. Appl.* **2014**, *3*, 1−7.
(10) Kumakura, K.; Nakakoshi, K.; Kishida, M.; Motohisa, J.; Fukui, T.; Hasegawa, H. *J. Cryst. Growth* **1994**, *145*, 308−313.
(11) Noborisaka, J.; Motohisa, J.; Fukui, T. *Appl. Phys. Lett.* **2005**, *86*, 213102.
(12) Van Weert, M. H. M.; Akopian, N.; Kelkensberg, F.; Perinetti, U.; van Kouwen, M. P.; Rivas, J. G.; Borgström, M. T.; Algra, R. E.; Verheijen, M. A.; Bakkers, E. P. A. M.; Kouwenhoven, L. P.; Zwiller, V. *Small* **2009**, *5*, 2134−2138.
(13) Bleuse, J.; Claudon, J.; Creasey, M.; Malik, N. S.; Gérard, J.-M.; Maksymov, I.; Hugonin, J.-P.; Lalanne, P. *Phys. Rev. Lett.* **2011**, *106*, 103601.
(14) Friedler, I.; Sauvan, C.; Hugonin, J. P.; Lalanne, P.; Claudon, J.; Gérard, J. M. *Opt. Express* **2009**, *17*, 2095−2110.
(15) Lumerical Solutions Inc. http://www.lumerical.com/tcad-products/fdtd/ (accessed Jan 2015).